Revisiting Automated G-Protein Coupled Receptor Modeling: The Benefit of Additional Template Structures for a Neurokinin-1 Receptor Model

Benny Kneissl,[†,‡] Bettina Leonhardt,[†,§] Andreas Hildebrandt,[‡] and Christofer S. Tautermann*[,||]

Center for Bioinformatics, Saarland University, 66123 Saarbrücken, Germany, science + computing ag, 80807 München, Germany, Department of Lead Discovery, Boehringer-Ingelheim Pharma GmbH & Co. KG, 88397 Biberach, Germany

Received November 17, 2008

The feasibility of automated procedures for the modeling of G-protein coupled receptors (GPCR) is investigated on the example of the human neurokinin-1 (NK1) receptor. We use a combined method of homology modeling and molecular docking and analyze the information content of the resulting docking complexes regarding the binding mode for further refinements. Moreover, we explore the impact of different template structures, the bovine rhodopsin structure, the human β_2 adrenergic receptor, and in particular a combination of both templates to include backbone flexibility in the target conformational space. Our results for NK1 modeling demonstrate that model selection from a set of decoys can in general not solely rely on docking experiments but still requires additional mutagenesis data. However, an enrichment factor of 2.6 in a nearly fully automated approach indicates that reasonable models can be created automatically if both available templates are used for model construction. Thus, the recently resolved GPCR structures open new ways to improve the model building fundamentally.

Introduction

G-protein coupled receptors (GPCRs[a]) represent the largest family of signal transducing membrane proteins in the human genome. More than 800 GPCRs, divided into five main classes by the so-called GRAFS system,[1] have been determined.[2] Although they all share a common structural feature, the presence of seven transmembrane helices, the sequence similarity is low throughout the whole phylogenetic tree. Nevertheless, some conserved residues and motifs have been identified.[3−7]

The functions of GPCRs vary as much as their sequences do. Among others, they are involved in biological processes like blood pressure regulation, immune responses, or processing light and smell impulses.[8,9] Today, it is known that the perturbation of GPCR function may result in severe diseases like diabetes, cancer, central nervous system disorders, and many more.[10,11] Hence, GPCRs are very interesting targets for the pharmaceutical industry and, consequently, about 50% of the drugs currently on the market and 25% among the top-selling drugs target GPCRs.[12,13]

Despite the great relevance of GPCRs for many biological processes, there is only little structural information available at atomic level due to the difficulties in crystallization and the size of these proteins. So far, only four GPCR structures have been resolved at atomic resolution and three of them even no more than a few months ago.[14−17] Hence, computer-aided methods for the prediction of GPCR structures become increasingly important. The approaches available today can roughly be divided into two classes: ab initio methods, where the structure is solely predicted from the sequence[18−20] and approaches based on homology or comparative modeling, where at least one known structure of a homologous receptor is required as a template for model building.

In this study, we focus on comparative modeling approaches, which have successfully been applied to different globular[21] as well as membrane proteins.[22,23] The general idea is based on the observation that three-dimensional structures of proteins are typically more conserved than their amino acid sequences.[24] Consequently, proteins with homologous sequences are expected to show a similar three-dimensional structure. In general, comparative modeling consists of four steps: template selection, sequence alignment, model building, and model validation.[25]

In a recent study, Nowak and co-workers extended this general framework by a molecular docking step to improve and facilitate the model building and validation process.[26] After generating a large amount of models by an automated procedure to sample the side chain conformational space, a potent ligand was docked to all models to identify those side chain conformations of the binding site that are advantageous for ligand binding. Afterward, the information of the docking runs was used to fine-tune a new set of models by restricting the determined residues to appropriate positions during the model building process. The ligand was docked in the new model set, and the ligand−receptor complexes were evaluated based on the CScore, which was used to finally determine a set of best fitting models, re-entering the docking procedure with 30 ligands. Despite some manual refinements following afterward, the top-scoring ligand−receptor complexes already revealed the general binding motifs of the serotonin 5-HT_{1A} receptor. With this approach, Nowak et al. successfully modeled this aminergic receptor, yielding impressive results in terms of high enrichment factors in virtual screening approaches. Remarkably, no additional experimental information, e.g., from mutagenesis studies, has been used in the first steps of this procedure. In our opinion, this is currently one of the most promising methods for approaching automated modeling of G-protein coupled receptors.

* To whom correspondence should be addressed. Phone: +49 (7351) 54-94030. Fax: +49 (7531) 83-94030. E-mail: christofer.tautermann@boehringer-ingelheim.com.

† These authors contributed equally to this work.

‡ Center for Bioinformatics, Saarland University.

§ science + computing ag.

|| Department of Lead Discovery, Boehringer-Ingelheim Pharma GmbH & Co. KG.

[a] Abbreviations: GPCR, G-protein coupled receptor; NK1, neurokinin-1; $5HT_{1A}$, 5-hydroxytryptamine (serotonin) receptor 1A; EL2, extracellular loop 2; TM, transmembrane.

10.1021/jm8014487 CCC: $40.75
Published on Web 04/28/2009

Here, we apply Nowak's method to the human neurokinin-1 (NK1) receptor, a member of the neurokinin receptor family. The natural ligands of this family, the neurokinins, also termed as tachykinins, are small neuropeptides that are widely distributed within the peripheral and central nervous systems and are involved in neurotransmission and neuromodulation. Studies suggest that they are involved in various inflammatory and immune diseases.[27,28] Therefore, many antagonists targeting the NK receptors have been developed as therapeutic agents.[29]

Evers and Klebe already developed a homology model of the NK1 receptor based on the structure of bovine rhodopsin,[30] which was suitable to identify a novel submicromolar antagonist by virtual screening. Similar to the approach of Nowak, they started with a large number of initial models and used ligand information from a docking run to further improve the models. However, Evers and Klebe used more prior knowledge, e.g., about the conformation of the ligand, from the beginning. They assumed that the bioactive conformation is identical with its geometry in solid state and hence performed a rigid docking. In addition, they evaluated the docking complexes based on interactions derived from mutagenesis data rather than the corresponding docking score. Thus, the approach of Klebe and Evers requires strong manual interaction during the model building and refinement process, whereas we want to judge the feasibility of highly automated approaches to GPCR modeling.

Therefore, we explore if the procedure by Nowak et al. is generally transferable to nonaminergic GPCR modeling to yield suitable initial models for further refinement steps in reasonable time and with reasonable effort. Considering that this approach has originally been applied to an aminergic receptor (5-HT_{1A}), we expect significantly more intrinsic difficulties in our case because NK1 belongs to the group of peptide binding receptors and the putative binding site of the endogenous ligand differs from the binding site of small molecule antagonists.

The second aim of our study is a deeper understanding of the influence of multiple different templates on the comparative modeling of GPCRs. Hence, we use the bovine rhodopsin structure and the recently resolved human β_2 adrenergic receptor structure as templates in the homology modeling step. Moreover, we combine both templates to extend the accessible conformational space, leading to larger backbone flexibility in the model building, not investigated in aforementioned studies. We assume that we can improve our models using multiple templates in an automated fashion. The final evaluation of the models is based on virtual screening techniques on a data set compiled from the literature as well as in house molecules.

Methods

Software. All homology models presented in this work were generated using MODELLER 8v2, an established standard for comparative modeling.[31] MOE 2007.09 (Molecular Operating Environment) was used for the alignments as well as manually refinements of the models.[32] The protein−ligand docking was performed using Glide (Grid-based Ligand Docking with Energetics) in SP mode.[33] The chemical compound was drawn using Symyx Draw.[34] The alignments were formatted and represented using ALSCRIPT,[35] the graphics containing 3D structures were generated with BALLView,[36] the molecular viewer and modeling tool of the Biochemical Algorithms Library BALL,[37] version 1.2, and the enrichment plots were created with the statistical program tool R.[38]

Alignments. We computed the pairwise alignments of the human NK1 receptor sequence (UniProt ID P25103) first with bovine rhodopsin (PDB ID 1F88) and second with the human β_2 adrenergic receptor (PDB ID 2RH1, removing the lysozyme fusion protein) denoting the resulting alignments as R1 and B1, respectively. To study the impact of related sequences on the alignment, we also performed a multiple alignment of the human NK1 receptor with the human NK2 (UniProt ID P21452) and human NK3 (UniProt ID P29371) sequence. The result was then aligned with the bovine rhodopsin sequence (called R123). Repeating the procedure with the human β_2 adrenergic receptor did not change the results of the B1 alignment. Furthermore, we carried out a multiple alignment of the human NK1 sequence with both the human β_2 adrenergic receptor and bovine rhodopsin (called RB1). All alignments were computed in MOE using a gap start penalty of 7.0 and a gap extension cost of 1.0. Because of the low sequence similarity, we decided to use the BLOSUM 30 substitution matrix. We checked the plausibility of each alignment on both the mapping of conserved motifs and residues of class rhodopsin-like GPCRs as well as the number of gaps appearing in helical regions, manually adjusting unfavorably aligned regions. The residues proposed to be involved in the binding mode are additionally denoted using the Ballesteros−Weinstein nomenclature.[39]

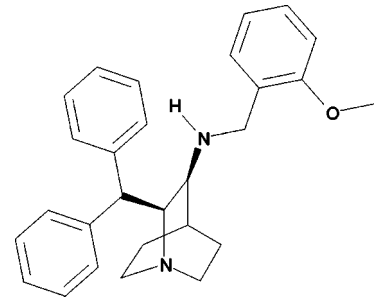

Figure 1. Structure of the quinuclidine amine **1** (CP-96345).[41]

Model Generation. For each alignment, 300 homology models were generated by employing MODELLER,[26] using the structure of bovine rhodopsin (1F88) and/or the human β_2 adrenergic receptor (2RH1) as templates. From the sequence alignment of the target protein and known template structures, MODELLER derives restraints expressed in terms of conditional probability functions (pdfs) for the target protein.[40] Optimizing the placement of the target protein coordinates in the molecular pdf with a conjugate gradient algorithm in combination with some nondeterministic steps, the program obtains slightly different models for the same alignment. Thus, the generation of a large number of models ensures a thorough sampling of the conformational space of the side chains of the receptor. Employing more than one template increases backbone flexibility and thus expanding the accessible conformational space.

Docking. The potent nonpeptide NK1 antagonist CP-96345[41] **1** (cf. Figure 1) was flexibly docked into all generated models using Glide in SP mode. Glide first produces a rough initial guess to reduce the search space, followed by a torsion-angle optimization of the most promising initial candidates. The best results of this second stage are then refined by a Monte Carlo method to produce the predicted docking pose.[42] Finally, the best docking pose based on the Glide-score is chosen. Prior to docking, the ligand was optimized with the MMFF94 force field in MOE.

Model Refinements. Following the approach of Nowak, we examined the top scoring docking poses to identify the essential key interactions that could be used to guide the model refinement. As shown in the Result and Discussion section in detail, none of such interactions could be found prevalent in the top scoring docking poses. Thus, we had to visually inspect the docking results, taking further knowledge from mutagenesis studies into account. The most reliable suggestions concerning the binding mode propose a H-bond between the exocyclic secondary amine to Gln 165 (4.60) and an interaction between His 197 (5.39) and the benzhydryl group.[29,41,43−46] These findings from mutagenesis experiments are now taken as a substitute for the information, which was gained in the study by Nowak et al. by the first docking runs.

In a first refinement step, we restrained the χ_1 angle and the χ_2 angle of Gln 165 (4.60) to −60° and to 170°, respectively, to ensure its proper orientation into the binding pocket. The interaction between His 197 (5.39) and **1** as well as the π-stacking between

Tyr 272 (6.59) and His 197 (5.39) as suggested by mutagenesis experiments was strengthened by a clockwise rotation of helix 5 by 30° (seen from extracellular side) in the bovine rhodopsin template.

To further follow the approach by Nowak, we selected 14 conformationally diverse models from the restrained model set and docked a balanced set of 50 highly ($IC_{50} < 1\ \mu M$) and weakly ($IC_{50} > 10\ \mu M$) active NK1 ligands taken from the public database AurSCOPE to determine the most useful model for the identification of active ligands by docking. Unfortunately, but not unexpected, there was no model that separates the two groups satisfactorily. The failure of all models to separate the ligand groups can be attributed to the kind of interactions involved in the binding mode as well as the quite small activity difference for both ligand sets. Thus, the docking scores and also visual inspection did not give us additional information, which can be used for model improvement, and therefore we skipped further studies on multiple ligands, which is also in line with our aim to model GPCRs as automated as possible.

In a second refinement step manual changes, i.e., manual side chain placement of the binding site residues of three models followed and the selection process will be described in the next chapters. To relax the conformation of the generated docking poses, we performed an energy minimization of the side chain atoms employing the AMBER99 force field as implemented in MOE. The backbone atoms of the modified residues and the ligand atoms were kept fixed during this relaxation. Thereafter, we performed an energy minimization of the entire binding pocket and the docked ligand using the MMFF94 force field. All these refinement steps were done in MOE with default parameters.

Virtual Screening. For the virtual screening, we combined public domain ligands from the database AurSCOPE GPCR (company Aureus Pharma) and in house data of Boehringer Ingelheim to a set of 1784 molecules including 58 active ones. Active molecules are defined to have an IC_{50} value lower than 1 μM and all inactive ones have an IC_{50} value larger than 10 μM. The set was balanced among others with respect to the average molecular weight (actives: 463.7 Da; inactives: 425.5 Da) as well as average charge (0.414, 0.407) and the average number of rotatable bonds (6.88, 7.06) to minimize the influences of these parameters. The protonation states of the compounds were assigned using MOE, and the compounds were energy minimized with the MMFF94 force field before docking. The virtual screening was done with GLIDE in SP mode using default parameters and the enrichment plots were generated using R.

Results and Discussion

Alignment Study. The overall sequence identity of the human NK1 receptor with bovine rhodopsin and with the human β_2 adrenergic receptor is lower than 30%. In this range, the number of alignment errors increases rapidly, resulting in the most substantial origin of errors in comparative modeling.[47] However, class I GPCRs share some highly conserved residues and motifs such that an unambiguous alignment can be achieved.[3−7] In all four alignments (see Figure 2 and Table 1), the conserved residues and motifs are correctly aligned, resulting in a proper arrangement of the seven helical regions. Moreover, 30 residues forming the general binding cavity for ligands identified by Rognan et al.[48] in an extensive study of 369 nonolifactory human GPCR sequences are also correspondingly aligned in all four cases. The alignment of the binding site residues of the human NK1 receptor proposed by the interaction model of Evers and Klebe, namely Gln 165, Glu 193, His 197, Ile 204, His 265, and Tyr 272, agrees with their published alignment,[30] except in the alignment R1. In this alignment, Tyr 272 (6.59) was mapped on Tyr 274 (6.57) of the bovine rhodopsin structure instead of the neighbored residue Phe 276 (6.59). This mapping was achieved by the insertion of a gap into the helical region. In our opinion, inserting gaps in structurally conserved regions is highly unlikely and indicates that a family alignment (as in the case of the multiple alignment R123) gives more reasonable results.

Structure Study. To obtain reasonable orientations of the binding site residues in the homology model, these residues need to be mapped on residues of the template structure that are pointing into the binding pocket. As mentioned before the essential NK1 residues for binding of **1** affirmed by various mutagenesis studies are Gln 165 (4.60) and His 197 (5.39).[44,45] Examining our alignments with bovine rhodopsin, these amino acids are mapped to Pro 171 (4.60) and Val 204 (5.39), respectively. Both residues are oriented into the binding pocket, and thus the alignment seems to be reasonable in this region. In the case of the human β_2 adrenergic receptor, the previously mentioned amino acids are mapped to Pro 168 (4.60) and to Ala 200 (5.39). While the latter is directed toward the binding pocket, the position of Pro 168 (4.60) does not seem to be suitable because it is oriented toward the neighbored helix 5. However, the positions of its neighbors Lys 167 (4.59) and Ile 169 (4.61) are even less appropriate. Altogether, we suppose that the orientation of helix 4 in rhodopsin seems to be a more suitable template than helix 4 of the human β_2 receptor. For helix 5, however, the opposite holds regarding the corresponding residues to His 197 and Ile 204 (see Table 2). Hence, we expected that a model generated by the combination of both templates and thus including backbone flexibility will perform best in the virtual screening experiment.

In the case of the pairwise alignment R1, the mapping of Tyr 272 in NK1 to Tyr 274 (6.57) in rhodopsin is less reasonable than the mapping to Phe 276 (6.59) as in the case of the multiple alignment because it is directed away from the TM cavity. Thus, we skipped the alignment R1 in the further modeling steps. Other residues being involved in the binding mode denoted by Evers and Klebe are Glu 193 (5.35), Ile 204 (5.46), and His 265 (6.52).[30] Table 2 lists the corresponding residues, which are all pointing well into the TM cavity (cf. Figure 3).

In addition, we examined the position of the extracellular loop 2 (EL2) in the two template structures carefully because it is described in other studies that the EL2 of rhodopsin causes many difficulties in the docking process.[30,50] Following the approach of Nowak, this extracellular loop was cut out of the homology model in a preprocessing step to ensure a successful protein−ligand docking. In contrast, the EL2 of the human β_2 adrenergic receptor is located well above the TM cavity, forming a short helix rather than a β-hairpin. Hence, we did not expect significant difficulties caused by the EL2 in the docking step. Consequently, we have cut out the EL2 only in the homology models that are exclusively based on the template structure of bovine rhodopsin (alignment R123).

Docking. One of the best studied ligands for the NK1 receptor is **1**, and thus we used it for our first docking run into our initial models (Table 3, no. 1). Mutagenesis studies suggest that Gln 165 on helix 4 forms a hydrogen bond with the exocyclic secondary amine.[44] Furthermore, the binding affinity is negatively affected as soon as His 197 is mutated to alanine. The analysis of a series of **1** analogues identified the benzhydryl group as the binding partner.[45] Besides these two residues, various assumptions about other residues being involved in the binding mode, e.g., Glu 193, Ile 204, His 265, and Tyr 272, have been published.[29,30,46]

Because one of our aims was to test the general applicability of automated modeling procedures for nonaminergic GPCRs, we sorted the models according to their docking score of the

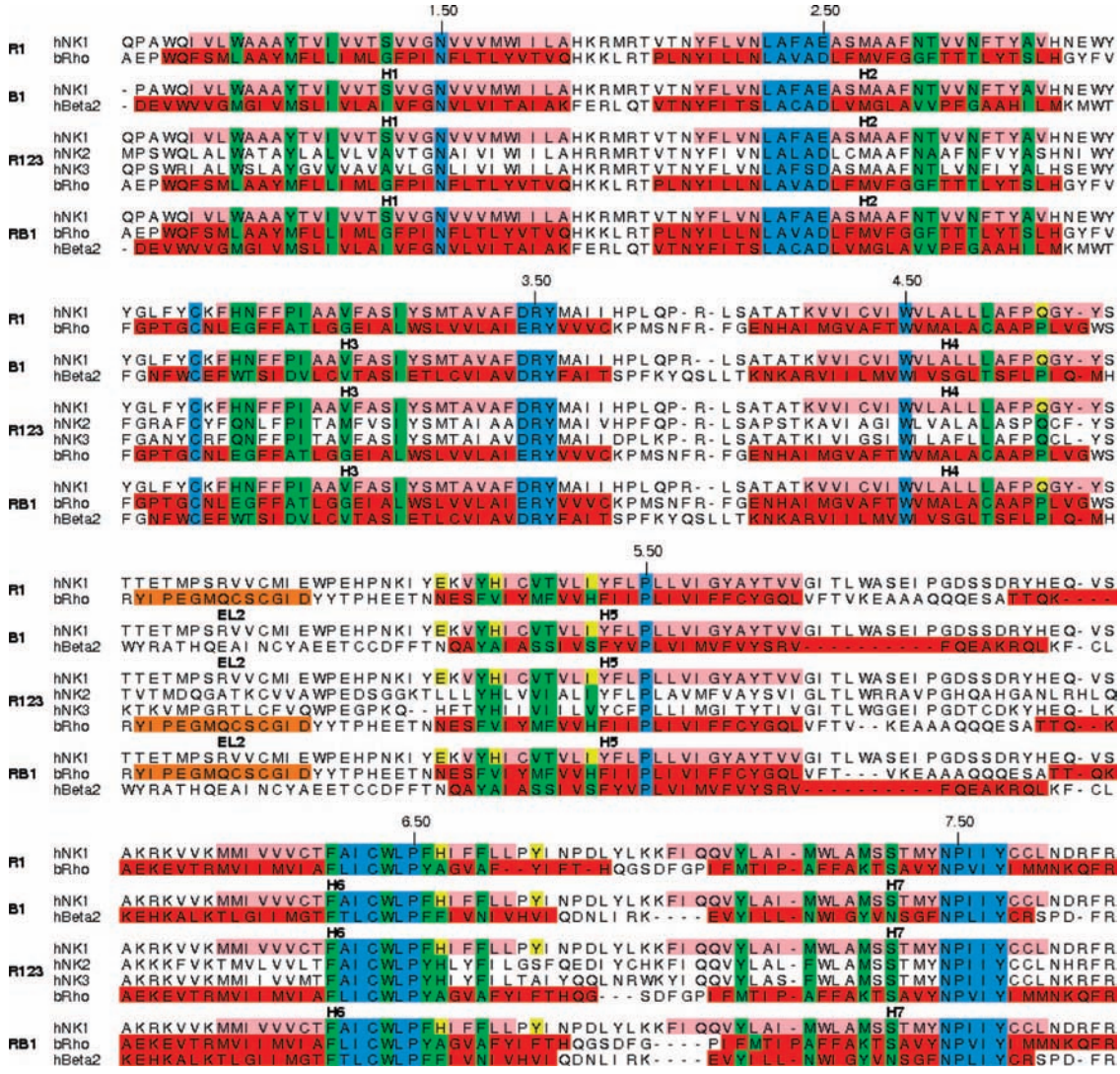

Figure 2. Sequence alignments used for model generation: First, the pairwise alignment of the human NK1 receptor and bovine rhodopsin (R1). Second, the pairwise alignment of the human NK1 receptor and the human β2 adrenergic receptor (B1). Third, the multiple alignment of the human NK1−3 receptors and bovine rhodopsin (R123). Fourth, the multiple alignment of the human NK1 receptor, bovine rhodopsin, and the human β2 adrenergic receptor (RB1). The red and orange marked regions are the TM helices of both templates and the EL2 of the rhodopsin structure, respectively. The light-red marked regions indicate the TM helices of the human NK1 receptor predicted by TMpred.[49] Blue marked residues are conserved residues/motifs of class I GPCRs. Residues forming the TM cavity are marked in green.[48] All binding site residues of the human NK1 receptor, proposed by Evers and Klebe,[30] are colored in yellow. The alignments were formatted using ALSCRIPT.[35]

Table 1. The Four Alignments Used in This Work[a]

name	used sequences
R1	human NK1 and bovine rhodopsin
B1	human NK1 and human β_2 adrenergic receptor
R123	human NK1, human NK2, human NK3, and bovine rhodopsin
RB1	human NK1, bovine rhodopsin, and human β_2 adrenergic receptor

[a] The names are composed of the used template structures bovine rhodopsin (R) and human β_2 adrenergic receptor (B) as well as the number of the human neurokinin receptor (1−3).

Table 2. The Mapping of the NK1 Residues Involved in the Binding Mode of Ligand **1** and Their Corresponding Amino Acids Based on the Different Alignments

NK 1	bovine rhodopsin (R123)	human β_2 adrenergic receptor (B1)	bovine rhodopsin (R1)
Gln 165 (4.60)	Pro 171 (4.60)	Pro 168 (4.60)	Pro 171 (4.60)
Glu 193 (5.35)	Asn 200 (5.35)	Asn 196 (5.35)	Asn 200 (5.35)
His 197 (5.39)	Val 204 (5.39)	Ala 200 (5.39)	Val 204 (5.39)
Ile 204 (5.46)	His 211 (5.46)	Ser 207 (5.46)	His 211 (5.46)
His 265 (6.52)	Ala 269 (6.52)	Phe 290 (6.52)	Ala 269 (6.52)
Tyr 272 (6.59)	Phe 276 (6.59)	Val 297 (6.59)	Tyr 274 (6.57)

best scoring pose as done by Nowak.[26] However, we could not identify essential key interactions in the docking complexes that could be used to guide the model refinement by investigating the models and the corresponding score. Hence, solely from the docking pose and score, it is not possible to distinguish between reasonable and unreasonable homology models. We suppose that the reason for this result might be the different types of interactions. Nowak et al. modeled the serotonin 5-HT_{1A} receptor, where strong interactions like salt bridges between the ligand and the receptor were formed during the docking procedure. In contrast, ligand binding in the human NK1-receptor involves only weaker interactions like hydrogen bonds or aromatic interactions. The scoring functions for docking do not seem to be sufficiently sensitive to properly rank these kinds of interactions, such that the score is not a good indicator for the quality of the docking poses in this case. Moreover, small changes in the conformation can yield large binding energy differences,[51] and because the scoring functions are adjusted based on the crystal structures, homology models perform in

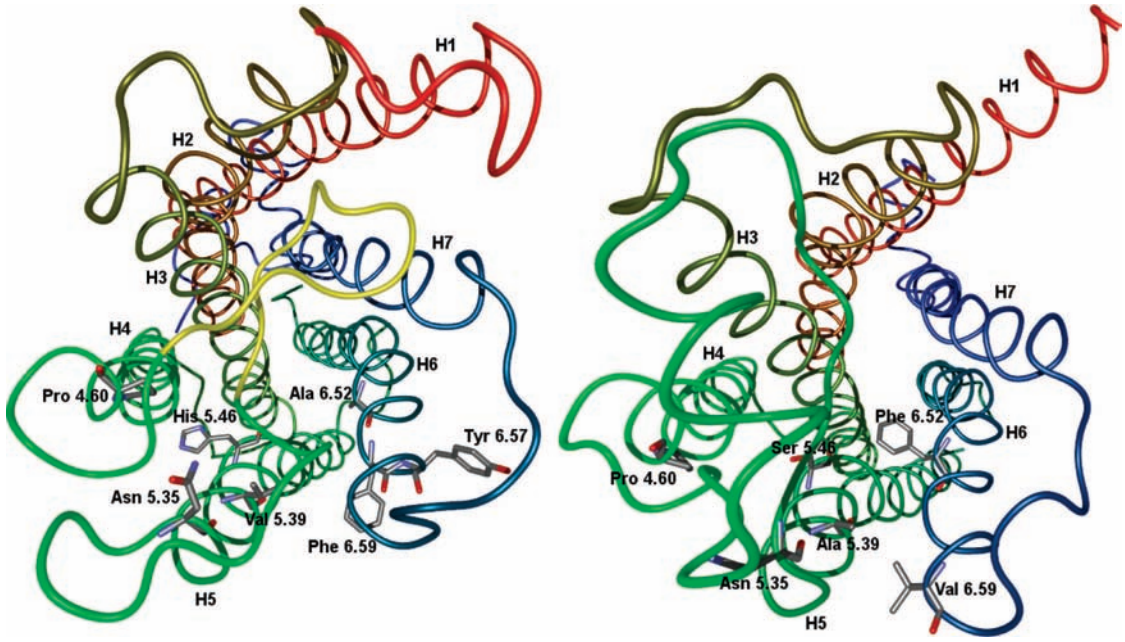

Figure 3. On the left side the template structure of bovine rhodopsin and on the right side the structure of the human β2 receptor is represented. The removed EL2 of the bovine rhodopsin structure is marked in yellow. All residues corresponding to the binding partners, proposed by Klebe, based on the alignments R123 (left) and B1 (right) are shown.

Table 3. All Model Types Generated in the Modelling Procedure

no.	name	alignment	template	restraints/refinements
1	INIT	R123	1F88	cut out EL2
2	REST	R123	1F88	cut out EL2 Gln 165: χ_1 angle = −60°, χ_2 angle = 170°
3	ROTA	R123	1F88 (rotated helix 5 by 30° clockwise)	cut out EL2 Gln 165: χ_1 angle = −60°, χ_2 angle = 170°
4	BETA	B1	2RH1	none
5	BOTH	RB1	1F88 + 2RH1	none
6	MO_INIT	R123	1F88	cut out EL2 manually optimized binding pocket
7	MO_REST	R123	1F88	cut out EL2 Gln 165: χ_1 angle = −60°, χ_2 angle = 170° manually optimized binding pocket
8	MO_ROTA	R123	1F88 (rotated helix 5 by 30° clockwise)	cut out EL2 Gln 165: χ_1 angle = −60°, χ_2 angle = 170° manually optimized binding pocket
9	CONS	R123	1F88 (rotated helix 5 by 30° clockwise)	majority vote of 14 selected models
10	DEST	R123	1F88	cut out EL2 manually destroyed binding pocket
11	RAND	R123	1F88	cut out EL2

many cases worse than the corresponding crystal structures, especially if no strong interaction is involved in the binding mode. Therefore, the poses have to be inspected visually using additional experimental information, e.g., from mutagenesis studies as described in the next section.

Model Refinements. Because the automated docking runs failed to identify crucial interactions between **1** and the receptor, we were forced to include mutagenesis data in the following refinement steps. We focused on the key interaction for binding **1**, a hydrogen bond between Gln 165 (4.60) and the exocyclic secondary amine of **1** as well as an aromatic interaction between His 197 (5.39) and the benzhydryl group of **1**.

The first step was to reject all models, which do not agree with the mutagenesis studies. To this end, we used two simple filtering criteria: a distance filter between the Cδ of Gln 165 (4.60) and the exocyclic secondary amine of **1** and a distance filter between the Cγ of His 197 (5.39) and the carbon atom of **1** connecting the two benzene rings. Combined, these two filters reduced the overall number of models based solely on bovine rhodopsin (R123) to approximately 4% of all complexes. Although a distance filter of 5 Å and 7.5 Å, respectively, is very coarse, visual inspection confirmed that both residues point into the binding pocket and particularly to their postulated binding partners.

Closer inspection also showed that in the remaining models, the torsion angles of Gln 165 (4.60) have values of $\chi_1 = -60°$ ($\pm 5°$) and $\chi_2 = 170°$ ($\pm 5°$). Thus, according to the original approach of Nowak, we constrained these angles for a new model generation run to optimize the distance to the binding partner of **1** (Table 3, no. 2). In the case of His 197 (5.39), we decided to modify the corresponding helix in the rhodopsin template by a clockwise rotation of 30°. This step was introduced to achieve both a strengthening of the interaction with **1** and to facilitate the formation of the π-stacking. Although this means a drastic change of the conformation, it has been shown by Vaidehi and co-workers[52] that ligand induced changes of the backbone are quite usual. We decided to rotate the helix directly in the template instead of postprocessing the generated

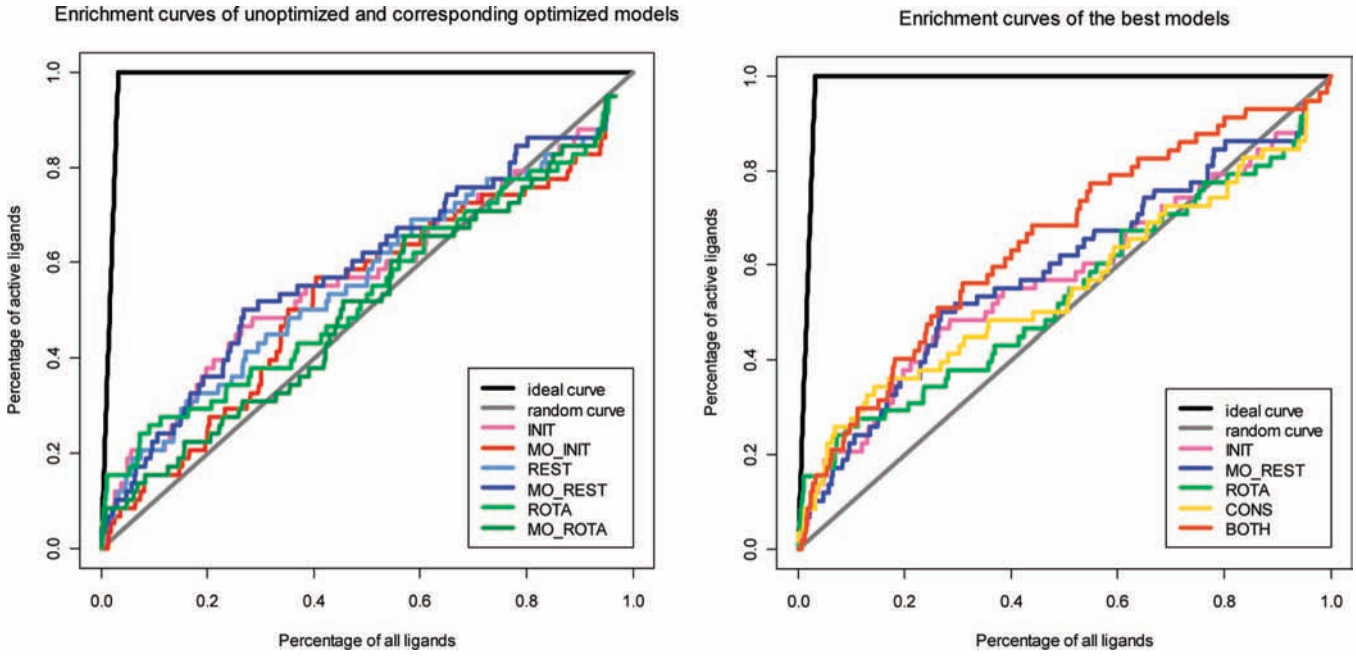

Figure 4. On the left the enrichment curves of the nonoptimized models and the corresponding manually optimized ones are shown. The figure on the right shows enrichment curves of the best models using the rhodopsin structure, the model using both templates, and the consensus model.

models to avoid clashes in the postprocessing procedure. In these models, which are based on the modified template structure, we restrained the torsion angles of Gln 165 (4.60) as described above, too (Table 3, no. 3). This manual modification of the template, however, is not in the main focus of this study, which is the test of an automated GPCR modeling and virtual screening procedure. The modification of the template was done manually according to mutagenesis data, and therefore this technique may yield GPCR models closer to reality but is not suitable for an automated approach.

For the 300 models based on the human β_2 adrenergic receptor (B1, RB1), we were not able to identify common side chain features. In both cases, we used the above-mentioned distance filters to reject those models, which do not agree with the mutagenesis studies. However, only few of the models fulfill the filter criteria (<1%). In particular, for the models based on the aligment RB1, the backbones of the models vary too much such that a restraint or other modifications can not be applied to continue with a model refinement. For the subsequent virtual screening experiment, we selected from both model sets (Table 3, nos. 4 and 5) by visual inspection a model among the top 10 scored complexes showing reasonable orientation of residues Gln 165 (4.60) and His 197 (5.39).

In a second refinement step, we selected from the pool of all generated models based on the R123 alignment 14 models manually. The selection was guided by the ability of various models to accommodate some public domain ligands as taken from the Aureus database. The models were picked according to reasonable docking poses and conformational diversity of amino acid residues close to the active site. To test the influence of the modeling techniques so far we selected three of these 14 models, one belonging to the INIT, one to the REST, and one to the ROTA model set (Table 3, nos. 6−8) to improve their interactions manually. This is not in line with an automated modeling process, but it will give us information about the general suitability of the various approaches for model generation so far.

Finally, we built a consensus model of all these 14 selected models (Table 3, no. 9). To this end, we took the backbone of a ROTA model and manually adjusted the conformation of the binding site residues to the conformation that occurs in the majority of all complexes, a procedure which is in line with an automated modeling process.

Virtual Screening. A virtual screening experiment was performed on a total of 11 different models (Table 3). Our two negative controls, an arbitrarily chosen model (RAND) from the INIT model set and a model with a "destroyed" pocket (DEST) by manually manipulating the side chains such that they fill the binding site, worked as expected because no enrichment could be found (data not shown). Particularly, in the case of the model DEST (manually closed pocket), only a small amount was able to be docked into the binding pocket by GLIDE. Although more ligands (about two-third) could be docked into the model RAND, the enrichment factor is lower than random for this model.

Next, we compared the enrichment curves of the three nonoptimized models (nos. 1−3) with their corresponding manually optimized ones (nos. 6−8) (left picture in Figure 4). Although we expected an improvement, the manually optimized models yield a lower enrichment factor in two of the three cases. The reason for this effect depends on the optimization process itself and may be attributed to overfitting: since we improved these models manually to strengthen the contact between the important side chain residues and **1**, we simultaneously may have reduced the possible interactions to other ligands not taken into account. This led to a worse result in the virtual screening.

The analysis of the enrichment curves of the three other models (CONS, BETA, and BOTH) shows interesting results (right picture in Figure 4). In contrast to the manual refinements, the CONS model improved the results noticeable. Hence, the combination of the best side chain conformations is a reasonable step in model tuning. Its enrichment factor of the top 10% equals 2.6, which is in agreement with other virtual screening experiments of nonaminergic GPCR models.[53]

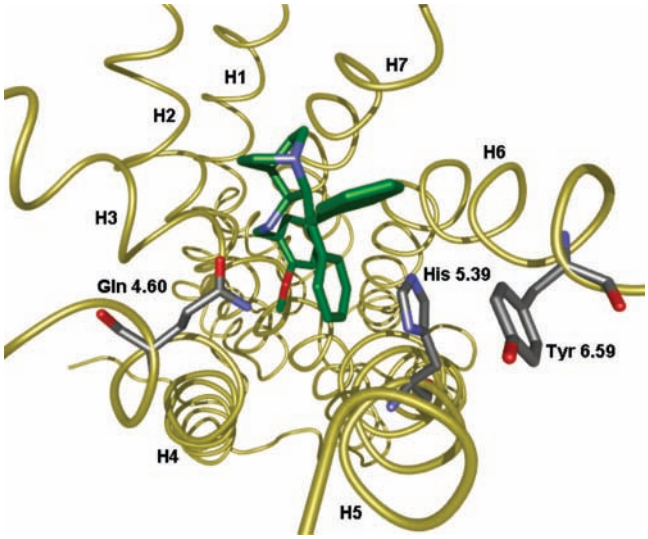

Figure 5. Backbone representation of the best model using two template. For a better view, we cut out the EL2. The interactions with the two important residues Gln 165 (4.60) and His 197 (5.39) are accentuated.

For the models based on β_2, we also expected an improvement for two reasons. First, the position of the EL2 well above the transmembrane regions and, second, the appropriate orientation of helix 5. But the enrichment factor is surprisingly lower than random (curve not shown). We suppose that especially the position of Gln 165 on helix 4 might be crucial for the binding, but in this region, the β_2 adrenergic receptor is unsuitable as discussed in the section Structure Study. However, using the combination of the two templates β2 and rhodopsin (BOTH), the enrichment curve equals the one of the consensus model and is in most cases even better (right picture in Figure 4). Remembering that this model was straightforwardly generated, e.g., without cutting out EL2 or any refinement steps, this is a remarkable result. Most steps were performed automatically using scripting languages with the only (important) exception of the choice of the model out of the 300 generated. This manual effort was, however, negligible, because we have only looked at the models with the 10 best docking scores. Hence, in this case, the docking score guided us to find a reasonable model efficiently, although we were not able to discover important side chain conformations for further refinement steps as shown by Nowak et al.

In Figure 5, we represent the backbone of the model BOTH used in the virtual screening experiment. Here, the advantages of both templates are combined. First, the discussed positions of Gln 165 (4.60) and His 197 (5.39) are directed well into the binding pocket and, second, the previously mentioned π-stacking between Tyr 272 (6.59) and His 197 (5.39) is formed.

This result sheds light on the invaluable information the GPCR modeling community has gained by the resolution of the β_2 receptor and will gain by every newly emerging GPCR crystal structure.

Conclusion

In this study, we have investigated to which extent automated modeling of GPCRs is possible. Therefore, we followed the first modeling steps described by Nowak and co-workers. In our opinion, this is the most promising approach to improve homology models on an automated basis. We have thus attempted first to employ the approach to the modeling of the human NK1 based on the bovine rhodopsin template structure.

However, we soon found that this approach does not work for the nonaminergic case: our experiments found no essential key interactions in docking runs that could be used to guide the model refinement. We suggest that the reason for this insufficient result lies in the different type of interactions because in NK1 modeling no strong interactions such as salt bridges are involved in binding. In particular, aromatic interactions do not seem to be parametrized in an optimal way in current scoring functions and are therefore hard to identify. The high flexibility of **1** complicated the docking procedure additionally. Hence, we had to include additional experimental information derived from mutagenesis studies from the very beginning. The refinements, especially the rotation of helix 5 in the bovine rhodopsin structure, improved the results significantly. This shows that for modeling GPCRs, we still rely on experimental data to generate promising models.

Employing the human β_2 adrenergic receptor as a single template, however, yielded unsatisfying results, such that even a manual refinement based on the docking results was not feasible. Nonetheless, the combination of both available templates (rhodopsin and β_2) and the resulting expansion of the backbone conformational space for model building yields an enrichment factor in the range of the manually constructed consensus model. This was achieved without further refinements and just by choosing one of the top scoring docking complexes of **1**, whose side chain orientations are confirmed by experimental data. Thus, we suggest that the usage of multiple templates improves the models in a constitutive way. Hence, the human β_2 adrenergic receptor and probably also the other recently crystallized structures are very valuable for the homology model building of GPCRs. This shows that the availability of more structures improves the model building process because a larger conformational space, in particular in backbone regions, can be sampled. Using homology modeling in combination with docking, however, seems to be a viable option for automated receptor modeling if an essential very strong interaction between the ligand and the receptor is postulated, as in the case of amine receptors or fatty acid receptors.

Concluding our study, we suppose that data from mutagenesis studies must still be used to guide through the refinement steps of initial GPCR models. However, we suggest that these models should be generated based on multiple templates to include backbone flexibility. Hence, the crystallization of further GPCR structures has opened new ways to improve GPCR model building significantly.

Acknowledgment. Benny Kneissl and Bettina Leonhardt thank Boehringer Ingelheim Pharma GmbH & Co. KG for financial support of this study.

Supporting Information Available: Structures of compounds used for virtual screening. This material is available free of charge via the Internet at http://pubs.acs.org.

References

(1) Fredriksson, R.; Lagerstrom, M. C.; Lundin, L. G.; Schioth, H. B. The G-protein-coupled receptors in the human genome form five main families. Phylogenetic analysis, paralogon groups, and fingerprints. *Mol. Pharmacol.* **2003**, *63* (6), 1256–1272.
(2) Marchese, A.; George, S. R.; Kolakowski, L. F.; Lynch, K. R.; O'Dowd, B. F. Novel GPCRs and their endogenous ligands: expanding the boundaries of physiology and pharmacology. *Trends Pharmacol. Sci.* **1999**, *20* (9), 370–375.
(3) Attwood, T. K.; Findlay, J. B. C. Fingerprinting G-protein-coupled receptors. *Protein Eng.* **1994**, *7* (2), 195–203.
(4) Menzaghi, F.; Behan, D. P.; Chalmers, D. T. Constitutively activated G protein-coupled receptors: a novel approach to CNS drug discovery. *Curr Drug Targets* **2002**, *1* (1), 105–121.

(5) Fanelli, F.; De Benedetti, P. G. Computational modeling approaches to structure−function analysis of G protein-coupled receptors. *Chem. Rev.* **2005**, *105* (9), 3297–3351.
(6) Mirzadegan, T.; Benko, G.; Filipek, S.; Palczewski, K. Sequence analyses of G-protein-coupled receptors: Similarities to rhodopsin. *Biochemistry* **2003**, *42* (10), 2759–2767.
(7) Baldwin, J. M.; Schertler, G. F. X.; Unger, V. M. An alpha-carbon template for the transmembrane helices in the rhodopsin family of G-protein-coupled receptors. *J. Mol. Biol.* **1997**, *272* (1), 144–164.
(8) Hamm, H. E. The many faces of G protein signaling. *J. Biol. Chem.* **1998**, *273* (2), 669–672.
(9) Marinissen, M. J.; Gutkind, J. S. G-protein-coupled receptors and signaling networks: emerging paradigms. *Trends Pharmacol. Sci.* **2001**, *22* (7), 368–376.
(10) Dorsam, R. T.; Gutkind, J. S. G-protein-coupled receptors and cancer. *Nat. Rev. Cancer* **2007**, *7* (2), 79–94.
(11) Filmore, D. It's a GPCR world. *Modern Drug Discovery* **2004**, *7* (11), 24–28.
(12) Lundstrom, K. Latest development in drug discovery on G protein-coupled receptors. *Curr. Protein Pept. Sci.* **2006**, *7* (5), 465–470.
(13) Klabunde, T.; Hessler, G. Drug design strategies for targeting G-protein-coupled receptors. *ChemBioChem* **2002**, *3* (10), 929–944.
(14) Palczewski, K.; Kumasaka, T.; Hori, T.; Behnke, C. A.; Motoshima, H.; Fox, B. A.; Le Trong, I.; Teller, D. C.; Okada, T.; Stenkamp, R. E.; Yamamoto, M.; Miyano, M. Crystal structure of rhodopsin: A G protein-coupled receptor. *Science* **2000**, *289* (5480), 739–745.
(15) Murakami, M.; Kouyama, T. Crystal structure of squid rhodopsin. *Nature (London)* **2008**, *453*, 363–367.
(16) Rasmussen, S. G. F.; Choi, H. J.; Rosenbaum, D. M.; Kobilka, T. S.; Thian, F. S.; Edwards, P. C.; Burghammer, M.; Ratnala, V. R. P.; Sanishvili, R.; Fischetti, R. F.; Schertler, G. F. X.; Weis, W. I.; Kobilka, B. K. Crystal structure of the human beta(2) adrenergic G-protein-coupled receptor. *Nature (London)* **2007**, *450*, 383–387.
(17) Warne, T.; Serrano-Vega, M. J.; Baker, J. G.; Moukhametzianov, R.; Edwards, P. C.; Henderson, R.; Leslie, A. G. W.; Tate, C. G.; Schertler, G. F. X. Structure of a beta(1)-adrenergic G-protein-coupled receptor. *Nature (London)* **2008**, *454*, 486–491.
(18) Shacham, S.; Topf, M.; Avisar, N.; Glaser, F.; Marantz, Y.; Bar-Haim, S.; Noiman, S.; Naor, Z.; Becker, O. M. Modeling the 3D structure of GPCRs from sequence. *Med. Res. Rev.* **2001**, *21* (5), 472–483.
(19) Shacham, S.; Marantz, Y.; Bar-Haim, S.; Kalid, O.; Warshaviak, D.; Avisar, N.; Inbal, B.; Heifetz, A.; Fichman, M.; Topf, M.; Naor, Z.; Noiman, S.; Becker, O. M. PREDICT modeling and in silico screening for G-protein coupled receptors. *Proteins: Struct., Function, Bioinformatics* **2004**, *57* (1), 51–86.
(20) Trabanino, R. J.; Hall, S. E.; Vaidehi, N.; Floriano, W. B.; Kam, V. W. T.; Goddard, W. A. First principles predictions of the structure and function of G-protein-coupled receptors: validation for bovine rhodopsin. *Biophys. J.* **2004**, *86* (4), 1904–1921.
(21) Kopp, J.; Bordoli, L.; Battey, J. N. D.; Kiefer, F.; Schwede, T. Assessment of CASP7 predictions for template-based modeling targets. *Proteins* **2007**, *69* (Suppl. 8), 38–56.
(22) Martinelli, A.; Tuccinardi, T. An overview of recent developments in GPCR modelling: methods and validation. *Expert Opin. Drug Discovery* **2006**, *1* (5), 459–476.
(23) Filizola, E.; Filizola, M. Advances in the development and application of computational methodologies for structural modeling of G-protein-coupled receptors. *Expert Opin. Drug Discovery* **2008**, *3* (3), 343–355.
(24) Lesk, A. M.; Chothia, C. H. The response of protein structures to amino-acid-sequence changes. *Philos. Trans. R. Soc., A* **1986**, *317* (1540), 345–356.
(25) Marti-Renom, M. A.; Stuart, A. C.; Fiser, A.; Sanchez, R.; Melo, F.; Sali, A. Comparative protein structure modeling of genes and genomes. *Annu. Rev. Biophys. Biomol. Struct.* **2000**, *29*, 291–325.
(26) Nowak, M.; Kolaczkowski, M.; Pawlowski, M.; Bojarski, A. J. Homology modeling of the serotonin 5-HT1A receptor using automated docking of bioactive compounds with defined geometry. *J. Med. Chem.* **2006**, *49* (1), 205–214.
(27) Pennefather, J. N.; Lecci, A.; Candenas, M. L.; Patak, E.; Pinto, F. M.; Maggi, C. A. Tachykinins and tachykinin receptors: a growing family. *Life Sciences* **2004**, *74* (12), 1445–1463.
(28) Patacchini, R.; Maggi, C. A. Peripheral tachykinin receptors as targets for new drugs. *Eur. J. Pharmacol.* **2001**, *429* (1−3), 13–21.
(29) Cascieri, M. A.; Shiao, L. L.; Mills, S. G.; Maccoss, M.; Swain, C. J.; Yu, H.; Ber, E.; Sadowski, S.; Wu, M. T.; Strader, C. D.; Fong, T. M. Characterization of the interaction of diacylpiperazine antagonists with the human neurokinin-1 receptor−identification of a common binding-site for structurally dissimilar antagonists. *Mol. Pharmacol.* **1995**, *47* (4), 660–665.
(30) Evers, A.; Klebe, G. Successful virtual screening for a submicromolar antagonist of the neurokinin-1 receptor based on a ligand-supported homology model. *J. Med. Chem.* **2004**, *47* (22), 5381–5392.
(31) Eswar, N.; Webb, B.; Marti-Renom, M. A.; Madhusudhan, M. S.; EramianD. Shen, M.-y.; Pieper, U.; Sali, A. , Comparative Protein Structure Modeling Using Modeller In *Current Protocols in Bioinformatics*; John Wiley and Sons, Inc.: New York, 2006; Vol. 15.
(32) *MOE−Molecular Operating Environment*; Chemical Computing Group: Montreal, 2007.
(33) *GLIDE−Grid-based Ligand Docking with Energetics*; Schrödinger: New York, 2004.
(34) *Symyx Draw 3.1*; Symyx Technologies Inc.: Santa Clara, CA, 2008; http://www.symyx.com/.
(35) Barton, G. J. ALSCRIPT−a tool to format multiple sequence alignments. *Protein Eng.* **1993**, *6* (1), 37–40.
(36) Moll, A.; Hildebrandt, A.; Lenhof, H. P.; Kohlbacher, O. BALLView: An object-oriented molecular visualization and modeling framework. *J. Comput.-Aided Mol. Des.* **2005**, *19* (11), 791–800.
(37) Kohlbacher, O.; Lenhof, H. P. BALL−rapid software prototyping in computational molecular biology. *Bioinformatics* **2000**, *16* (9), 815–824.
(38) R Development Core Team. *R: A Language and Environment for Statistical Computing*, 2008; http://www.R-project.org.
(39) Ballesteros, J. A.; Weinstein, H. Integrated methods for the construction of three-dimensional models and computational probinf of structure function relations in G-protein-coupled receptors. *Neuroscience Methods* **1995**, *25*, 366–428.
(40) Sali, A.; Blundell, T. L. Comparative protein modeling by satisfaction of spatial restraints. *J. Mol. Biol.* **1993**, *234* (3), 779–815.
(41) Snider, R. M.; Constantine, J. W.; Lowe, J. A.; Longo, K. P.; Lebel, W. S.; Woody, H. A.; Drozda, S. E.; Desai, M. C.; Vinick, F. J.; Spencer, R. W.; Hess, H. J. A potent nonpeptide antagonist of the substance-P (NK1) receptor. *Science* **1991**, *251* (4992), 435–437.
(42) Friesner, R. A.; Banks, J. L.; Murphy, R. B.; Halgren, T. A.; Klicic, J. J.; Mainz, D. T.; Repasky, M. P.; Knoll, E. H.; Shelley, M.; Perry, J. K.; Shaw, D. E.; Francis, P.; Shenkin, P. S. Glide: A new approach for rapid, accurate docking and scoring. 1. Method and assessment of docking accuracy. *J. Med. Chem.* **2004**, *47* (7), 1739–1749.
(43) Fong, T. M.; Yu, H.; Huang, R. R. C.; Cascieri, M. A.; Swain, C. J. Relative contribution of polar interactions and conformational compatibility to the binding of neurokinin-1 receptor antagonists. *Mol. Pharmacol.* **1996**, *50* (6), 1605–1611.
(44) Fong, T. M.; Yu, H.; Cascieri, M. A.; Underwood, D.; Swain, C. J.; Strader, C. D. Interaction of Glutamine-165 in the 4th transmembrane segment of the human neurokinin-1 receptor with quinuclidine antagonists. *J. Biol. Chem.* **1994**, *269* (21), 14957–14961.
(45) Fong, T. M.; Cascieri, M. A.; Yu, H.; Bansal, A.; Swain, C.; Strader, C. D. Amino aromatic interaction between histidine-197 of the neurokinin-1 receptor and CP-96345. *Nature (London)* **1993**, *362* (6418), 350–353.
(46) Fong, T. M.; Yu, H.; Cascieri, M. A.; Underwood, D.; Swain, C. J.; Strader, C. D. The role of histidine-265 in antagonist binding to the neurokinin-1 receptor. *J. Biol. Chem.* **1994**, *269* (4), 2728–2732.
(47) Baker, D.; Sali, A. Protein structure prediction and structural genomics. *Science* **2001**, *294* (5540), 93–96.
(48) Surgand, J. S.; Rodrigo, J.; Kellenberger, E.; Rognan, D. A chemogenomic analysis of the transmembrane binding cavity of human G-protein-coupled receptors. *Proteins: Struct., Funct., Bioinf.* **2006**, *62* (2), 509–538.
(49) *TMPred Prediction of Transmembrane Regions and Orientation*; http://www.ch.embnet.org/software/TMPRED_form.html.
(50) Bissantz, C.; Bernard, P.; Hibert, M.; Rognan, D. Protein-based virtual screening of chemical databases. II. Are homology models of G-protein coupled receptors suitable targets. *Proteins: Struct., Funct., Genet.* **2003**, *50* (1), 5–25.
(51) Ferrara, P.; Jacoby, E. Evaluation of the utility of homology models in high throughput docking. *J. Mol. Model.* **2007**, *13*, 897–905.
(52) Bhattacharya, S.; Hall, S. E.; Li, H.; Vaidehi, N. Ligand-stabilized conformational states of human beta(2) adrenergic receptor: Insight into G-protein-coupled receptor activation. *Biophys. J.* **2008**, *94*, 2027–2042.
(53) Bissantz, C.; Schalon, C.; Guba, W.; Stahl, M. Focused library design in GPCR projects on the example of 5-HT2c agonists: Comparison of structure-based virtual screening with ligand-based search methods. *Proteins: Struct., Funct., Bioinf.* **2005**, *61* (4), 938–952.

JM8014487